

New metal-rich mixed chalcogenides with an intergrowth structure: $\text{Ni}_{5.68}\text{SiSe}_2$, $\text{Ni}_{5.46}\text{GeSe}_2$, and $\text{Ni}_{5.42}\text{GeTe}_2$ *

A. A. Isaeva,^a A. I. Baranov,^{a,b} Th. Doert,^c M. Ruck,^c V. A. Kulbachinskii,^d R. A. Lunin,^d and B. A. Popovkin^{e*}

^aDepartment of Materials Science, M. V. Lomonosov Moscow State University,
 1 Leninskie Gory, 119992 Moscow, Russian Federation.

Fax: +7 (495) 939 0998. E-mail: isaeva@inorg.chem.msu.ru

^bMax Planck Institute for Chemical Physics of Solids,
 Noethnitzer Strasse 40, 01187, Dresden, Germany.**

Fax: +49 (351) 464 63002. E-mail: baranov@cpfs.mpg.de

^cDresden University of Technology, Institute of Inorganic Chemistry,
 Helmholtzstrasse 10, D-01062 Dresden, Germany

Fax: +49 (351) 463 37287. E-mail: Michael.Ruck@chemie.tu-dresden.de***

^dDepartment of Physics, M. V. Lomonosov Moscow State University,
 1 Leninskie Gory, 119992 Moscow, Russian Federation.

Fax: +7 (495) 932 8876. E-mail: kulb@mig.phys.msu.ru

^eDepartment of Chemistry, M. V. Lomonosov Moscow State University,
 1 Leninskie Gory, 119992 Moscow, Russian Federation.

Fax: +7 (495) 939 0998. E-mail: popovkin@inorg.chem.msu.ru

New metal-rich mixed nickel–silicon and nickel–germanium chalcogenides, $\text{Ni}_{5.68}\text{SiSe}_2$, $\text{Ni}_{5.46}\text{GeSe}_2$, and $\text{Ni}_{5.42}\text{GeTe}_2$, were synthesized by high-temperature ceramic techniques. The X-ray diffraction study of single crystals grown from a molten flux revealed that the compounds are isostructural and crystallize in the tetragonal system (space group $I4/mmm$, $Z = 2$). These compounds are the first members of the family of $\text{M}_{7-8}\text{EX}_2$ -type ($\text{M} = \text{Ni}$ or Pd ; $\text{E} = \text{Sn}$ or Sb ; X is chalcogen) intergrowth structures containing "light" p elements E . Resistivity measurements on pressed textured pellets showed that both selenides are anisotropic metallic conductors in the directions parallel and perpendicular to the heterometallic bond systems. The geometric criteria of stability of the intergrowth structure type under consideration are discussed.

Key words: nickel, germanium, silicon, metal-rich chalcogenides, intergrowth structures, crystal structure, anisotropy of conductivity.

One of the structure types, in which metal-rich mixed chalcogenides containing low-dimensional infinite bond systems between transition and main-group metals can crystallize, includes compounds of the general formula $\text{M}_{7-8}\text{EX}_2$, where M is a transition metal, E is a main-group metal, and X is a chalcogen. The crystallographic data for the following representatives of this structure type were published so far: $\text{Ni}_{5.72(3)}\text{SbSe}_2$, $\text{Ni}_{5.66(2)}\text{SbTe}_2$,¹ $\text{Ni}_{5.98(3)}\text{SnS}_2$,² $\text{Ni}_{5.62(1)}\text{SnSe}_2$, $\text{Ni}_{5.78(2)}\text{SnTe}_2$,³ and $\text{Pd}_{6.21(1)}\text{SnTe}_2$.⁴

All these compounds crystallize in the tetragonal system (space group $I4/mmm$) and are built of the following two types of 2D slabs, which alternate along the c axis and have an interface consisting of M atoms: heterometallic slabs ${}^2_{\infty}[\text{M}_3\text{E}]$ of the slightly distorted Cu_3Au type and d -metal-chalcogenide slabs ${}^2_{\infty}[\text{M}_{4-8}\text{X}_2]$. In all known phases, except for $\text{Ni}_{5.98(3)}\text{SnS}_2$, the latter slabs can be considered as Cu_2Sb -type fragments. In the $\text{Ni}_{5.98(3)}\text{SnS}_2$ compound, the Cu_2Sb -type slabs randomly alternate with the antifluorite-type nickel-chalcogenide slabs.

All known phases of this family are nonstoichiometric with respect to d metal due to the fractional occupation of the M site in d -metal-chalcogenide slabs. The index 7 in the chemical formulas corresponds to the full occupancy of the site. The above-mentioned compositions of the compounds were refined in the course of the crystal structure solution and were verified by the energy dispersive

* Dedicated to Academician G. A. Abakumov on the occasion of his 70th birthday.

** Max-Planck-Institut für Chemische Physik fester Stoffe, Noethnitzer Strasse, 40, 01187, Dresden, Germany.

*** Technische Universität Dresden, Institut für Anorganische Chemie, Helmholtzstraße, 10, D-01062, Dresden, Germany.

X-ray analysis. Earlier, we have also demonstrated that the crystal structures of $\text{Pd}_{6.21(1)}\text{SnTe}_2$ (see Ref. 4) and $\text{Ni}_{5.78(2)}\text{SnTe}_2$ (see Ref. 5) are modulated, the appearance of the modulation waves being associated with the ordering of transition metal atoms in the partially occupied site.

The quantum chemical calculations of the difference charge density distributions in the model compounds with the compositions Ni_6SnS_2 (see Ref. 2) and $\text{Ni}_{5.75}\text{SnSe}_2$ (see Ref. 3) revealed the difference in the nature of chemical bonding in two types of slabs. The heterometallic slabs are characterized by multicenter interactions, whereas pairwise interactions are present in the *d*-metal-chalcogenide slabs. The anisotropy of chemical bonding predicted by the calculations was experimentally confirmed by the anisotropy of the metallic conductivity measured in different directions on a pressed powder of $\text{Ni}_{5.62(1)}\text{SnSe}_2$ (see Ref. 3) and a single crystal of $\text{Ni}_{5.78(2)}\text{SnTe}_2$.⁵ The Pauli paramagnetism found in the $\text{Ni}_{5.66(2)}\text{SbTe}_2$,¹ $\text{Ni}_{5.62(1)}\text{SnSe}_2$, and $\text{Ni}_{5.78(2)}\text{SnTe}_2$ compounds³ is also consistent with the results of quantum chemical calculations.

Only antimony and tin were known as *p* metals that form compounds of this structure type. This contribution presents our attempt to answer the question whether the corresponding mixed selenides and tellurides do exist for lighter Group 14 elements (germanium and silicon). It is known that the intergrowth structures of interest are not formed with *p* metals heavier than Sn and Sb. The phase equilibria studies in the ternary systems $\text{Ni}-\text{E}-\text{X}$ ($\text{E} = \text{Pb}$ or Bi ; $\text{X} = \text{S}$, Se , or Te)^{6–9} revealed no compounds with the composition $\text{Ni}_{7-8}\text{EX}_2$. In the nickel-rich parts of these systems, the following mixed chalcogenides were found: $\text{Ni}_3\text{Pb}_2\text{S}_2$,¹⁰ $\text{Ni}_3\text{Pb}_2\text{Se}_2$ (shandite structure),¹¹ $\text{Ni}_3\text{Bi}_2\text{S}_2$,^{6,12} $\text{Ni}_3\text{Bi}_2\text{Se}_2$ (parkerite structure),⁶ the $\text{Ni}_{151.5}\text{Pb}_{24}\text{S}_{92}$ phase that has no isostructural analogs^{7,8} and is built of a three-dimensional framework of homo- and heterometallic bonds, and the Ni_6BiS_3 and $\text{Ni}_{11}\text{Bi}_5\text{S}_4$ phases,^{6,9} whose crystal structures remain unknown. We found no published data on the synthesis of any phases of the structure types under consideration for Ge and Si.

In the present study, we report the synthesis and structural characterization of new metal-rich mixed nickel–silicon and nickel–germanium chalcogenides with the compositions $\text{Ni}_{5.68}\text{SiSe}_2$, $\text{Ni}_{5.46}\text{GeSe}_2$, and $\text{Ni}_{5.42}\text{GeTe}_2$. These are the first representatives of the $\text{Ni}_{7-8}\text{EX}_2$ family containing "light" *p* elements.

Results and Discussion

All reflections in the X-ray powder diffraction patterns of repeatedly annealed equilibrium samples with the compositions $7 \text{ Ni} + \text{Ge/Si} + 2 \text{ Se}$ and $7 \text{ Ni} + \text{Ge} + 2 \text{ Te}$ (see the Experimental section), except for a few weak reflections assigned to a small amount of a nickel metal admixture, were indexed in I-centered tetragonal unit

Table 1. EDX results for the crystals of ternary compounds

System	Ni	Si/Ge (wt.%)	Se/Te	Calculated formula
Ni–Si–Se	65(1)	5(1)	29(1)	$\text{Ni}_{5.9}\text{SiSe}_2$
Ni–Ge–Se	61(1)	12(3)	29(1)	$\text{Ni}_{5.7}\text{GeSe}_2$
Ni–Ge–Te	47(1)	12(1)	41(1)	Ni_5GeTe_2

cells with the parameters similar to those of $\text{Ni}_{5.62}\text{SnSe}_2$ and $\text{Ni}_{5.78}\text{SnTe}_2$, respectively. According to the X-ray powder diffraction data, all samples with the composition $7 \text{ Ni} + \text{Si} + 2 \text{ Te}$, which were synthesized from different starting reagents under different conditions, were composed of known binary compounds and nickel. The single crystals of three new compounds were studied by energy dispersive X-ray analysis and used for the crystal structure determination.

The elemental analysis of the single crystals showed (Table 1) that the new ternary phases have compositions similar to those of the known phases of this type, all three new phases being also nonstoichiometric with respect to nickel. Table 2 gives the crystallographic data and the refinement statistics for the crystal structures of the new compounds. The occupancy of the Ni(3) site (see the positional and anisotropic thermal parameters of the atoms in Tables 3 and 4) was allowed to vary and appeared to be partial in all structures. The crystal structure refinements with anisotropic displacement parameters based on all independent reflections converged to the compositions $\text{Ni}_{5.68(1)}\text{SiSe}_2$, $\text{Ni}_{5.46(1)}\text{GeSe}_2$, and $\text{Ni}_{5.42(1)}\text{GeTe}_2$, respectively.*

To verify the validity of the compositions determined from the structural data, samples with the stoichiometries $\text{Ni}_{5.68}\text{SiSe}_2$, $\text{Ni}_{5.46}\text{GeSe}_2$, and $\text{Ni}_{5.42}\text{GeTe}_2$ were prepared from mixtures of the corresponding elements and annealed in evacuated quartz ampoules at 650 °C for 60 days with four intermediate grindings. As a result, phase-pure samples containing no nickel impurities (X-ray powder diffraction data) were obtained.

Crystal structures. All three compounds are isostructural with the $\text{Ni}_{5.72(3)}\text{SbSe}_2$, $\text{Ni}_{5.66(2)}\text{SbTe}_2$, $\text{Ni}_{5.62(1)}\text{SnSe}_2$, $\text{Ni}_{5.78(2)}\text{SnTe}_2$, and $\text{Pd}_{6.21(1)}\text{SnTe}_2$ compounds. In their structures (Fig. 1), the following two types of 2D slabs alternate along the *c* axis: slightly distorted Cu_3Au -type fragments with the composition ${}^2_{\infty}[\text{Ni}_3\text{E}]$ ($\text{E} = \text{Si}$ or Ge) and defected Cu_2Sb -type fragments with the partially occupied metal site and the composition ${}^2_{\infty}[\text{Ni}_{4-8}\text{X}_2]$ ($\delta = 1.32$ for $\text{Ni}_{5.68}\text{SiSe}_2$; $\delta = 1.54$ for

* Additional information on the X-ray diffraction experiments can be obtained from the Fachinformationszentrum Karlsruhe, 76344 Eggenstein-Leopoldshafen, Germany (Fax: (+49) 7247 808 666. E-mail: crysdata@fiz-karlsruhe.de); the deposition numbers CSD-417880 ($\text{Ni}_{5.68}\text{SiSe}_2$), CSD-417878 ($\text{Ni}_{5.46}\text{GeSe}_2$), and CSD-417879 ($\text{Ni}_{5.42}\text{GeTe}_2$).

Table 2. Crystallographic data and the X-ray data collection and refinement statistics for Ni_{5.68(1)}SiSe₂, Ni_{5.46(1)}GeSe₂, and Ni_{5.42(1)}GeTe₂

Formula	Ni _{5.68(1)} SiSe ₂	Ni _{5.46(1)} GeSe ₂	Ni _{5.42(1)} GeTe ₂
Molecular weight/g mol ⁻¹	520.07	553.42	650.70
Crystal system		Tetragonal	
Space group		<i>I4/mmm</i> (№ 139)	
Unit cell parameters			
<i>a</i> /Å	3.576(1)	3.606(1)	3.688(1)
<i>c</i> /Å	18.339(2)	18.276(5)	19.027(2)
<i>V</i> /Å ³	234.5(3)	237.63(7)	258.73(4)
<i>Z</i>	2	2	2
<i>T</i> /K	293	293	293
Crystal dimensions/mm	0.05×0.05×0.01	0.06×0.2×0.01	0.18×0.2×0.02
<i>d</i> _{calc} /g cm ³	7.37	7.73	8.35
μ/mm ⁻¹	37.98	42.70	36.20
Scanning mode	ω – 2θ	ω	ω
θ Scan range	4.45–27.48	2.23–30.44	4.28–31.82
Absorption correction	Semiempirical	Analytical	Analytical
Number of measured reflections	1937	1643	2370
<i>R</i> _{int}	0.0644	0.0383	0.0458
<i>R</i> _σ	0.0364	0.0148	0.0155
Number of independent reflections	110	146	174
Number of reflections with <i>I</i> ≥ 2σ(<i>I</i>)	108	137	174
Number of refined parameters	17	17	17
For reflections with <i>I</i> ≥ 2σ(<i>I</i>)			
<i>R</i> ₁	0.0302	0.0203	0.0229
<i>wR</i> ₂	0.0685	0.0539	0.0625
For all reflections			
<i>R</i> ₁	0.0305	0.0224	0.0229
<i>wR</i> ₂	0.0686	0.0553	0.0625
Weighting scheme*	1/[σ ² (<i>F</i> _o ²) + (0.0504 <i>P</i>) ² + + 0.4616 <i>P</i>]*	1/[σ ² (<i>F</i> _o ²) + + (0.0400 <i>P</i>) ²]*	1/[σ ² (<i>F</i> _o ²) + (0.0447 <i>P</i>) ² + + 1.2915 <i>P</i>]*
Residual electron density (max/min)/e Å ⁻³	1.07/–1.02	0.76/–0.66	1.40/–1.26
GOOF (based on all reflections)	1.11	1.27	1.13

* $P = (F_o^2 + 2F_c^2)/3$

Ni_{5.46}GeSe₂; δ = 1.58 for Ni_{5.42}GeTe₂). Each *d*-metal-chalcogenide slab, like those in other compounds belonging to the family under consideration, is related to the adjacent slab by a mirror plane located perpendicular to the *c* axis, resulting in the presence of two such slabs in the unit cell. According to the X-ray diffraction study of a single crystal of Ni_{5.46}GeSe₂ (space group *I4/mmm*, *a* = 3.599(1) Å, *c* = 18.279(5) Å at 140 K), the main reflections lying in the *ab** plane are accompanied by very weak satellites with *q*₁ ≈ 0.4*a** and *q*₂ ≈ 0.4*b**. This fact is indicative of the possible presence of modulations in the selenide structure analogous to those found earlier in the structures of mixed tellurides.^{3,5}

Table 5 gives selected interatomic distances and bond angles in the structures of the new compounds; the corresponding parameters for Ni_{5.62}SnSe₂ and Ni_{5.78}SnTe₂ (see Ref. 3) are given for comparison. The lengths of the heterobimetallic bonds are either very similar (Ni(1)–E) or slightly larger (Ni(2)–E) than those in the intermetal-

lic phases Ni₃Si (2.479 Å)¹³ and Ni₃Ge (2.526 Å).¹⁴ The lengths of the homometallic Ni–Ni bonds are, on the whole, substantially larger than those in nickel metal (2.489 Å)¹⁵ and are comparable with the corresponding bond lengths in the intermetallics Ni₃E and telluride Ni_{2.86}Te₂ (2.666 and 2.674 Å, respectively).¹⁶ The shortest Ni–Se distances (Ni(3)–Se bonds parallel to the *c* axis) are slightly shorter than those found in the binary selenides (*cf.*, 2.29–2.5 Å in Ni₃Se₂ (see Ref. 17) and 2.287 Å in Ni₆Se₅ (see Ref. 18)) but are comparable, like other Ni–Se distances, with the corresponding distances in Ni_{5.62}SnSe₂ (see Ref. 3) and Ni_{5.72}SbSe₂ (see Ref. 1). All Ni–Te distances in Ni_{5.42}GeTe₂ fall in the range characteristic of the analogous interactions in Ni_{2.86}Te₂ (see Ref. 16) (2.425, 2.582, and 2.677 Å) and are similar to the corresponding bond lengths in Ni_{5.78}SnTe₂ (see Ref. 3) and Ni_{5.66}SbTe₂ (see Ref. 1). In all structures, the E–E and X–X interatomic distances are larger than 3.6 Å, and, consequently, these interactions are nonbonding.

Table 3. Fractional atomic coordinates, occupancies, and equivalent displacement parameters for the $\text{Ni}_{5.68(1)}\text{SiSe}_2$, $\text{Ni}_{5.46(1)}\text{GeSe}_2$, and $\text{Ni}_{5.42(1)}\text{GeTe}_2$ structures

Atom	Wyckoff site	x/a	y/b	z/c	Occu- pancy	$U_{\text{eq}}^* \cdot 10^3 / \text{\AA}^2$
$\text{Ni}_{5.68(1)}\text{SiSe}_2$						
Si	2a	0	0	0	1	15.7(8)
Se	4e	1/2	1/2	0.17934(5)	1	19.0(4)
Ni(1)	8g	0	1/2	0.09297(5)	1	18.4(4)
Ni(2)	2b	1/2	1/2	0	1	17.5(5)
Ni(3)	4e	0	0	0.1984(2)	0.342(7)	22(1)
$\text{Ni}_{5.46(1)}\text{GeSe}_2$						
Ge	2a	0	0	0	1	10.6(3)
Se	4e	1/2	1/2	0.17960(3)	1	12.2(3)
Ni(1)	8g	0	1/2	0.09613(4)	1	11.9(3)
Ni(2)	2b	1/2	1/2	0	1	11.1(3)
Ni(3)	4e	0	0	0.1984(3)	0.232(5)	13(1)
$\text{Ni}_{5.42(1)}\text{GeTe}_2$						
Ge	2a	0	0	0	1	12.1(3)
Te	4e	1/2	1/2	0.17932(2)	1	13.4(2)
Ni(1)	8g	0	1/2	0.08875(3)	1	13.1(3)
Ni(2)	2b	1/2	1/2	0	1	13.1(3)
Ni(3)	4e	0	0	0.1904(3)	0.210(7)	14(2)

$$* U_{\text{eq}} = (U_{11}U_{22}U_{33})^{1/3}.$$

Conductivity. The results of conductivity measurements on pressed pellets of two new mixed selenides $\text{Ni}_{5.68}\text{SiSe}_2$ and $\text{Ni}_{5.46}\text{GeSe}_2$ are presented in Fig. 2, *a, b*. For both samples, the temperature dependences of the current run-

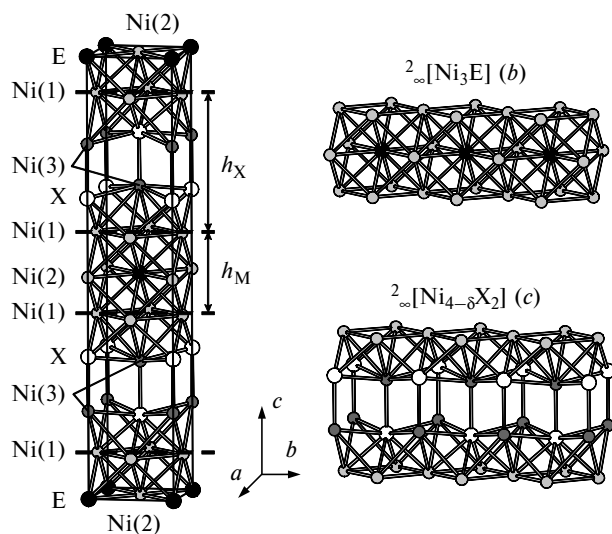


Fig. 1. Overall view of the crystal structure of $\text{Ni}_{7-8}\text{EX}_2$ ($\text{E} = \text{Si}$ or Ge ; $\text{X} = \text{Se}$ or Te) represented as a combination of the following two structural fragments: heterometallic Cu_3Au -type slabs (*b*, the height of the slab h_M) and Cu_2Sb -type *d*-metal-chalcogenide slabs (*c*, the height of the slab h_X). The interface between the slabs formed by a square-planar layer of $\text{Ni}(1)$ atoms is indicated by a dashed line. The unit cell is outlined. The $\text{Ni}(3)$ site is shown as completely occupied.

Table 4. Anisotropic displacement parameters* ($U_{ij} \cdot 10^3 / \text{\AA}^2$) for the $\text{Ni}_{5.68(1)}\text{SiSe}_2$, $\text{Ni}_{5.46(1)}\text{GeSe}_2$, and $\text{Ni}_{5.42(1)}\text{GeTe}_2$ structures ($U_{ij} = 0$)

Atom	U_{11}	U_{22}	U_{33}
$\text{Ni}_{5.68(1)}\text{SiSe}_2$			
Si	15.7(1)	15.7(1)	15.7(2)
Se	17.5(5)	17.5(5)	21.8(6)
Ni(1)	18.7(6)	15.5(6)	21.0(7)
Ni(2)	17.4(6)	17.4(6)	17.7(9)
Ni(3)	22.6(2)	22.6(2)	22(2)
$\text{Ni}_{5.46(1)}\text{GeSe}_2$			
Ge	10.0(3)	10.0(3)	11.9(5)
Se	11.8(3)	11.8(3)	13.1(4)
Ni(1)	12.3(4)	9.5(3)	13.9(4)
Ni(2)	11.2(4)	11.2(4)	10.8(6)
Ni(3)	15(1)	15(1)	11(2)
$\text{Ni}_{5.42(1)}\text{GeTe}_2$			
Ge	10.9(4)	10.9(4)	14.5(5)
Te	12.4(3)	12.4(3)	15.4(3)
Ni(1)	10.2(4)	13.4(4)	15.8(4)
Ni(2)	12.4(5)	12.4(5)	14.6(6)
Ni(3)	14(2)	14(2)	13(2)

$$* \exp[-2\pi^2(h^2a^2U_{11} + \dots + 2hkabU_{12} + \dots)].$$

ning parallel and perpendicular to the direction of pressing (ρ_{\perp} and ρ_{\parallel} , respectively) show that the resistivity decreases with decreasing temperature, which is typical of metallic conductors.

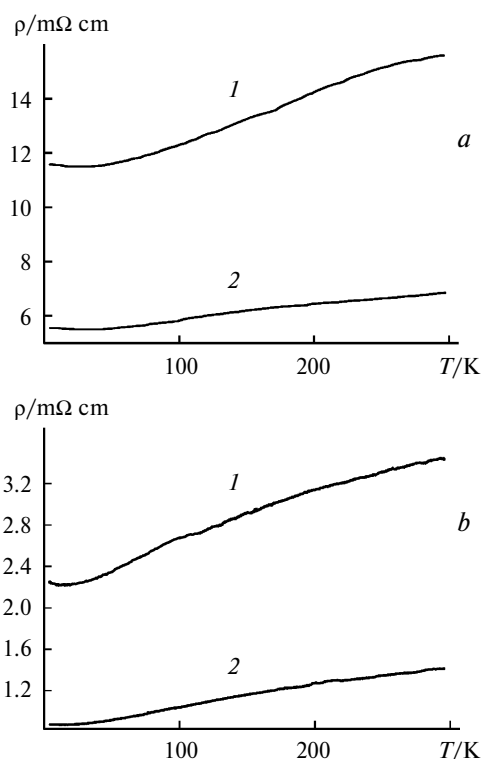
The X-ray powder diffraction studies of the pellet faces parallel and perpendicular to the direction of pressing revealed that both samples are texturized, like those investigated earlier.³ In the X-ray diffraction patterns for the faces perpendicular to the pressure direction, the intensities of the (00*l*) zone reflections are higher than those of the (*hk*0) zone reflections. To the contrary, the intensities of the (*hk*0) zone reflections are substantially higher in the X-ray diffraction patterns of the faces that are parallel to the pressure direction. This proves that crystallites in pressed pellets have the preferred orientation: their large faces are perpendicular to the direction of pressing. This fact provides a qualitative estimate of the anisotropy of the conductivity in the directions parallel and perpendicular to the heterometallic slabs. The results of measurements show that the resistivity along the slabs is substantially smaller than that in the lateral direction due to the good conductivity of the heterometallic fragments.

Therefore, our results show that the intergrowth structure under consideration is retained in three of four cases upon the substitution of tin in $\text{Ni}_{5.62(1)}\text{SnSe}_2$ and $\text{Ni}_{5.78(2)}\text{SnTe}_2$ with lighter isoelectronic germanium and silicon.

It is of interest to follow the changes in the unit cell parameters and the geometry of the structures caused by these substitutions. In the series $\text{Si} \rightarrow \text{Ge} \rightarrow \text{Sn}$, which can

Table 5. Selected interatomic distances and bond angles in the structures of selenides $\text{Ni}_{5.68}\text{SiSe}_2$, $\text{Ni}_{5.46}\text{GeSe}_2$, and $\text{Ni}_{5.62}\text{SnSe}_2$ and tellurides $\text{Ni}_{5.42}\text{GeTe}_2$ and $\text{Ni}_{5.78}\text{SnTe}_2$ (see Ref. 3)

Compound	$\text{Ni}_{5.68}\text{SiSe}_2$	$\text{Ni}_{5.46}\text{GeSe}_2$	$\text{Ni}_{5.62}\text{SnSe}_2$	$\text{Ni}_{5.42}\text{GeTe}_2$	$\text{Ni}_{5.78}\text{SnTe}_2$
Interatomic distances/Å					
Ni(1)—Ni(1)	2.529(1)	2.550(1)	2.6085(6)	2.608(1)	2.6644(4)
Ni(1)—Ni(2)	2.471(1)	2.517(1)	2.6362(9)	2.500(1)	2.624(1)
Ni(1)—Ni(3)	2.634(3)	2.597(3)	2.589(4)	2.672(4)	2.658(4)
Ni(1)—E	2.471(1)	2.517(1)	2.6362(9)	2.500(1)	2.624(1)
Ni(2)—E	2.529(1)	2.550(1)	2.6085(6)	2.608(1)	2.6644(4)
Ni(1)—X	2.389(1)	2.362(1)	2.374(1)	2.524(1)	2.536(1)
Ni(3)—X	2.241(4); 2.553(1)	2.230(5); 2.573(1)	2.245(6); 2.6283(9)	2.480(5); 2.616(1)	2.484(6); 2.6703(5)
Bond angles/deg					
Ni(1)—E—Ni(1)	61.56(1)	60.85(2)	59.31(2)	62.86(1)	61.03(3)
Ni(1)—E—Ni(2)	59.22(1)	59.573(8)	60.35(1)	58.570(6)	59.49(1)
Ni(1)—X—Ni(1)	63.91(2)	65.34(2)	66.64(4)	62.21(1)	63.36(3)
Ni(3)—X—Ni(3)	82.1(9)	82.3(1)	83.0(1)	85.4(1)	86.3(1)

**Fig. 2.** Temperature dependences of the resistivity measured on pressed pellets of $\text{Ni}_{5.68}\text{SiSe}_2$ (a) and $\text{Ni}_{5.46}\text{GeSe}_2$ (b) parallel (1) and perpendicular (2) to the pressure direction.

be considered for selenides, the parameter a , as expected, gradually increases, whereas the parameter c passes through a minimum (see Table 1; the unit cell parameters of $\text{Ni}_{5.62}\text{SnSe}_2$: $a = 3.6890(8)$ Å, $c = 18.648(3)$ Å). These dependences can be attributed to the necessity of the geometric matching of the nickel-selenide and heterometallic slabs, in which the site in the center is successively replaced by the p elements E increasing in size.

A comparison of the heights of two types of slabs (see Fig. 1) shows that the height of the heterometallic slab (h_M) increases in the series under consideration ($3.410(1) \rightarrow 3.514(1) \rightarrow 3.766(1)$ Å), whereas the height of the nickel-selenide slab (h_X) decreases ($5.760(1) \rightarrow 5.624(1) \rightarrow 5.558(1)$ Å). The mutual effect of these two factors results in the observed change in the unit cell parameter c . Evidently, as the heterometallic slab isometrically expands in the series of interest, the nickel-selenide slab has to be expanded in the ab plane with the simultaneous contraction along the c axis to retain the structure type. As can be seen from Table 5, this adjustment occurs through an elongation of the Ni(3)—X bonds lying nearly in the ab plane and an increase in the Ni(1)—X—Ni(1) angle. It should be noted that the Ni(3)—X bond lengths along the c axis, the Ni(1)—X distances, and the Ni(3)—X—Ni(3) bond angles remain virtually unchanged. Apparently, these parameters are determined primarily by the nature of the chalcogen, because they noticeably increase in going only from selenium to tellurium, the p element E being the same.

The above-described matching of the nickel-selenide slab by varying its geometric characteristics, in turn, provokes an additional distortion of the heterometallic fragments, which can be observed in the series $\text{Si} \rightarrow \text{Ge} \rightarrow \text{Sn}$ based on the decrease in the Ni(1)—E—Ni(1) bond angle. Therefore, both types of quasi-two-dimensional slabs match to each other thus forming the intergrowth structure.

The presence of the partially occupied Ni(3) site in the nickel-chalcogenide slabs characteristic of all known compounds $\text{M}_{7-8}\text{EX}_2$ can be caused by both the electronic factors and the necessity of the mutual geometric matching of two different types of quasi-two-dimensional slabs. No unambiguous relationships between the deviation from the stoichiometry with respect to d metal

and the nature of elements forming the compound were found. As can be seen from the series $\text{Ni}_{5.68}\text{SiSe}_2 \rightarrow \text{Ni}_{5.46}\text{GeSe}_2 \rightarrow \text{Ni}_{5.62}\text{SnSe}_2 \rightarrow \text{Ni}_{5.72}\text{SbSe}_2$ and $\text{Ni}_6\text{SnS}_2 \rightarrow \text{Ni}_{5.62}\text{SnSe}_2 \rightarrow \text{Ni}_{5.78}\text{SnTe}_2$, δ is not related in a simple way to the positions of the p element E and the chalcogen in the Periodic table on the condition that two other types of atoms in the compounds be the same.

The absence of compounds having crystal lattices of the specified type can be attributed both to the fact that the pairs of elements cannot, in principle, form Cu_3Au - and Cu_2Sb -type fragments and to the fact that two slabs cannot match to each other to form an intergrowth structure. In the Ni-Pb-X and Ni-Bi-X systems, compounds with this structure are absent due, apparently, to the fact that Cu_3Au -type slabs cannot be formed by these pairs of metals. In the hypothetical $\text{Ni}_{7-x}\text{PbX}_2$ and $\text{Ni}_{7-x}\text{BiX}_2$ compounds, the $\text{Ni}(1)\text{--Ni}(1)$ distances in the heterometallic slab, which should be equal to the $\text{Ni}(2)\text{--Pb}$ and $\text{Ni}(2)\text{--Bi}$ distances, respectively, according to the symmetry conditions, would be apparently too large for bonding distances. In particular, this is evident from a comparison of the typical Ni-Pb bond lengths (for example, 2.808 Å in $\text{Ni}_3\text{Pb}_2\text{Se}_2$ (see Ref. 11) and 2.889 Å in $\text{Ni}_{151.5}\text{Pb}_{24}\text{S}_{92}$ (see Ref. 8)) and the Ni-Bi bond lengths (2.696–2.959 Å in $\text{Ni}_3\text{Bi}_2\text{S}_2$ (see Ref. 12)) with the Ni-Ni bond length in nickel metal (2.489 Å). At the same time, the absence of this compound in the Ni-Si-Te system can be attributed to the fact that the slabs cannot match to each other. To match the nickel-chalcogenide slab that increases in size in going from $\text{Ni}_{5.68}\text{SiSe}_2$ to hypothetical telluride, the $\text{Ni}(2)\text{--Si}$ bond in the heterometallic slab should be substantially longer than 2.53 Å (see Table 5), which is apparently impossible for this pair of elements.

The intermetallics of the corresponding p and d metals in a ratio of 3 to 1 that belong to the Cu_3Au type or the similar Cu_3Ti type (for the Ni-Sb pair) are typical of all pairs of metals, which form known intergrowth compounds of the structure type under consideration.¹⁹ It is also known that nickel forms a Cu_2Sb -type structure with tellurium defected with respect to metal. Based on this fact, it can be concluded that a further search for new analogs of metal-rich chalcogenides with intergrowth structures should be performed only in systems containing pairs of d and p metals, which form intermetallics with the Cu_3Au -type or similar stoichiometry and structure (for example, the Cu-Si , Cu-Ge , Fe-Ga , Fe-Ge , Fe-Sn , Ni-Al , Ni-Ga , Ni-In , Pd-Pb , Pt-Al , Pt-Ga , Pt-In , Pt-Sn , and Pt-Pb pairs). However, the list of these pairs may be narrower because d metals should also be able to form stable crystalline fragments having a Cu_2Sb -type structure with other elements as well.

In our preliminary experiments, evidence confirming the existence of such intergrowth phases in the Ni-Ge-S , Ni-Si-S , Ni-As-Te , and Fe-Ge-Te systems was obtained.

Experimental

The samples were synthesized starting from the elements by high-temperature ceramic techniques. The thoroughly ground mixtures of the elements (Ni^* , Ge , Si , Te (all 99.99%), or Se (high-purity grade); the total weight of the sample was 1 g) corresponding to the stoichiometry Ni_7EX_2 ($E = \text{Si}$ or Ge ; $X = \text{Se}$ or Te) were placed in quartz ampoules with an inner diameter of 6 mm and a length of about 50 mm. Then the ampoules were sealed under vacuum ($\sim 5 \cdot 10^{-2}$ Torr), annealed at 540–650 °C for 14 days in CShOL 09 vertical furnaces controlled with PT200 temperature controllers with an accuracy of ± 3 °C, and water-quenched. According to the X-ray powder diffraction data, all samples consisted of four phases, and hence, the phase equilibrium was not achieved. The equilibrium samples containing only new compounds and nickel metal (according to the X-ray powder diffraction data) were obtained in the Ni-E-Se and Ni-Ge-Te systems only after the repeated annealing of pressed pellets (pressure load of about 2 tons) under the same conditions. The total time of annealing was 60 days for the silicon compound and 90 days for two germanium compounds. No new ternary compounds were found in the Ni-Si-Te system. Samples with the compositions $7 \text{ Ni} + \text{Si} + 2 \text{ Te}$ and $6 \text{ Ni} + \text{Si} + 2 \text{ Te}$ annealed over a long period of time (90 days) in the temperature range of 600–850 °C contained mixtures of the $\text{Ni}_{2.86}\text{Te}_2$, Ni_2Si , and Ni phases. We made an attempt to synthesize the hypothetical Ni_7SiTe_2 compound by annealing a mixture of the presynthesized compound Ni_3Si , Ni , and Te under the same conditions. However, we obtained only a mixture of known phases.

Single-crystal growth. Crystals of new compounds were grown from molten fluxes starting from PbCl_2 (reagent grade) (m.p. 501 °C)²⁰ for selenides or KI (reagent grade) (m.p. 679 °C)²¹ for telluride. Both salts were predried in air at 125 °C for 5 h in a drying oven. The stoichiometric mixtures (7 : 1 : 2) of the elements and the flux (total weight was $\sim 1\text{--}2$ g, the weight ratio of the charge to the flux was 1 : 1) were placed in cylindrical quartz ampoules (6×50 mm), which were then sealed under vacuum. The ampoules were heated to 850 °C for 12 h in a TG-1 shaft furnace controlled with a KPS-1-2MR temperature controller with an accuracy of ± 3 °C. Then the furnace was slowly cooled in an automatic mode to 500 °C at a rate of 1.5 deg h⁻¹. The cooling to room temperature was performed in the switched-off furnace. The samples were ground in a mortar and washed off from the flux by refluxing in hot water for 0.5–1 h. The washed samples contained small golden-colored crystals as thin elongated plates ($\sim 0.05 \times 0.03 \times 0.01$ mm).

X-ray powder diffraction analysis was performed on a Guinier–de Wolf camera FR-552 (Enraf-Nonius) using monochromated $\text{CuK}\alpha_1$ radiation. The X-ray diffraction patterns were analyzed with the use of the WinXPow program package and the PDF1 database (ICDD).²²

Energy dispersive X-ray analysis (EDX) of the crystals was carried out on a CAMEBAX SX-50 X-ray microanalyzer using the wavelength-dispersive technique. The maximum error of the determination was 3 wt.%. In most cases, the samples were prepolished with a diamond paste. The corresponding metal chalcogenides and pure metals were used as the reference

* A powder of nickel metal was prepurified from oxide by heating under a hydrogen stream at ~ 500 °C for 4 h.

samples. The experimental chemical compositions of the crystals were determined by averaging the data measured at several points on their surface.

X-ray diffraction study of nickel—silicon selenide was carried out on a KappaCCD (Nonius) single-crystal diffractometer using MoK α radiation ($\lambda = 0.71073$ Å) at 293 K; single crystals of nickel—germanium chalcogenides, on an image-plate diffractometer (Stoe IPDS II, MoK α) at 293 K. A single crystal of Ni_{5.46}GeSe₂ was additionally studied at 140 K to search for the satellite reflections indicative of the presence of the modulation waves in the structure. The unit cell parameters were determined from a set of several tens of reflection measured in the 2 θ -angle range from 5 to 90°. The exposure time per frame was 10–120 s. The systematic absences observed in the X-ray diffraction study indicated an I-centered lattice. To solve the crystal structures, the germanium and selenium sites were initially determined by the Patterson method (SHELXS-97).²³ Then the positions of the other atoms were localized and refined by repeated least-squares cycles and Fourier syntheses (SHELXL-97).²³ The absorption correction for Ni_{5.68}SiSe₂ was applied by the semiempirical method using the SCALEPACK program;²⁴ for Ni_{5.46}GeSe₂ and Ni_{5.42}GeTe₂, by the analytical method based on the refined crystal shape using the Stoe X-RED and X-SHAPE programs.²⁵ The final refinement of the crystal structures was carried out with anisotropic displacement parameters.

Conductivity measurements were carried out in the temperature range of 4.2–300 K on pressed rectangular pellets (10×5×5 mm) of the powdered pure compounds, which were prepared by annealing and pressed into pellets under ~4 tons. The standard four-probe technique was employed using the S3692 Acheson Silver DAG 1415 silver paste. The resistivity was measured along (ρ_{\parallel}) and perpendicular (ρ_{\perp}) to the direction of pressing. Crystallites of both phases are thin platelets and, consequently, their larger faces should be arranged perpendicular to the load direction.³ The electron diffraction study showed³ that the *c* axis is perpendicular to the larger face of the crystallites, resulting in the anisotropy of the conductivity of the pellets along different directions. To confirm the texturization of the samples, the X-ray powder diffraction study on a Bruker D8 Discover diffractometer equipped with a GADDS area detector (CuK α_1 radiation, reflection mode, pyrographite monochromator) was performed for the pellet faces parallel and perpendicular to the pressure direction.

We thank R. A. Sadykov (Institute for High Pressure Physics of the Russian Academy of Sciences, Troitsk, Russia) for measuring the X-ray diffraction patterns from faces of pressed samples.

This study was financially supported by the Russian Foundation for Basic Research (Project No. 06-03-32789) and the INTAS Fellowship Grant for Young Scientists (Grant No. 05-109-4795).

References

1. T. K. Reynolds, J. B. Bales, and F. J. DiSalvo, *Chem. Mater.*, 2002, **14**, 4746.
2. A. I. Baranov, A. A. Isaeva, L. Kloov, and B. A. Popovkin, *Inorg. Chem.*, 2003, **42**, 6667.
3. A. I. Baranov, A. A. Isaeva, L. Kloov, V. A. Kulbachinskii, R. A. Lunin, V. N. Nikiforov, and B. A. Popovkin, *J. Solid State Chem.*, 2004, **177**, 3616.
4. S. V. Savilov, A. N. Kuznetsov, B. A. Popovkin, V. N. Khrustalev, P. Simon, J. Getzschmann, Th. Doert, and M. Ruck, *Z. Anorg. Allg. Chem.*, 2005, **631**, 293.
5. A. A. Isaeva, A. I. Baranov, Th. Doert, V. A. Kulbachinskii, P. V. Gurin, V. G. Kytin, and V. I. Shtanov, *J. Solid State Chem.*, 2007, **180**, 221.
6. K. Mariolacos, *Chem. Erde*, 1987, **46**, 315.
7. K. Mariolacos, *Chem. Erde*, 1986, **45**, 338.
8. A. I. Baranov, A. A. Isaeva, B. A. Popovkin, and R. V. Shpanchenko, *Izv. Akad. Nauk SSSR, Ser. Khim.*, 2002, 1983 [*Russ. Chem. Bull., Int. Ed.*, 2002, **51**, 2139].
9. A. I. Baranov, Ph. D. (Chem.) Thesis, M. V. Lomonosov Moscow State University, Moscow, 2002, 156 pp. (in Russian).
10. M. A. Peacock and J. McAndrew, *Amer. Miner.*, 1950, **35**, 425.
11. A. Clauss, M. Warasteh, and K. Weber, *N. Jh. Miner. Mon.*, 1978, **6**, 256.
12. A. I. Baranov, A. V. Olenov, and B. A. Popovkin, *Izv. Akad. Nauk, Ser. Khim.*, 2001, 337 [*Russ. Chem. Bull., Int. Ed.*, 2001, **50**, 353].
13. Y. Oya and T. Suzuki, *Z. Metallkunde*, 1983, **74**, 21.
14. T. Suzuki, Y. Oya, and S. Ochiai, *Metallurgical Transactions A: Phys. Metallurgy and Mater. Sci.*, 1984, **15**, 173.
15. *ICSD Database, Version 1.0.0*, 2002, copyright by Fachinformationszentrum Karlsruhe, Germany.
16. R. B. Kok, G. A. Wieggers, and F. Jellinek, *Rec. Trav. Chim. Pays-Bas*, 1965, **84**, 1585.
17. J. P. Rouche and P. Lecocq, *C. R. Acad. Sci., Ser. C*, 1966, **262**, 555.
18. E. Rost and K. Haugsten, *Acta Chem. Scand.*, 1971, **25**, 3194.
19. *Diagrammy sostoyaniya dvoynykh metallicheskih sistem [Phase Diagrams of Binary Metal Systems]*, Ed. N. P. Lyakishev, Mashinostroenie, Moscow, 1999, **3**, Pt. 1 (in Russian).
20. G. G. Urazov and A. S. Karnankhov, *Dokl. Akad. Nauk SSSR*, 1954, **96**, 535 [*Dokl. Chem.*, 1954, **96** (Engl. Transl.)].
21. T. B. Massalski, *Binary Alloy Phase Diagrams*, 2nd ed., Ed. T. B. Massalski, ASM International, Materials park, Ohio, 1990, **3**, 2235.
22. *STOE WinXPow, Version 1.06*, 1999. STOE and Cie., GmbH.
23. (a) G. M. Sheldrick, *SHELXS-97, Program for crystal structure solution*, University of Göttingen, Göttingen (Germany), 1997; (b) G. M. Sheldrick, *SHELXL-97, Program for crystal structure refinement*, University of Göttingen, Göttingen (Germany), 1997.
24. (a) *SCALEPACK, Kappa CCD Software*. Nonius BV, Delft, The Netherlands, 1998; (b) Z. Otwinowski and W. Minor, in *Methods in Enzymology*, Eds C. W. Carter, Jr. and R. W. Sweet, Academic Press, New York, 1997, 276.
25. (a) *X-RED: Programm for Data Reduction and Absorption Correction*, STOE and Cie., Darmstadt, 2001; (b) *X-SHAPE: Crystal Optimisation for Numerical Absorption Correction*, STOE and Cie., Darmstadt, 1999.

Received January 26, 2007;
in revised form March 26, 2007